

Competition between pinning and melting in the two-dimensional vortex lattice

Ali Yazdani, C. M. Howald, W. R. White, M. R. Beasley, and A. Kapitulnik

Department of Applied Physics, Stanford University, Stanford, California 94305

(Received 8 June 1994; revised manuscript received 3 August 1994)

We discuss measurements of the ac complex conductance of *a*-MoGe films in the presence of a perpendicular magnetic field. The ac response of vortices in samples with weak pinning reveals an anomaly that is found to be consistent with a dislocation mediated melting in the two-dimensional vortex lattice on short length scales. However, increasing the effects of disorder on the vortex lattice by reducing the sample thickness leads to dominance of thermal-activated creep over melting. With increasing disorder, the length scale associated with the correlations in the vortex lattice is reduced and eventually the melting phenomenon disappears.

The interplay between thermal fluctuations, dimensionality, and disorder in the vortex state of type-II superconductors has been the subject of enormous research lately. The nature of the phase transitions by which the vortex lattice (VL) could melt into a vortex liquid is expected to be determined mainly by dimensionality and disorder.¹ For example, in the three-dimensional case, as often applied to the high- T_c superconductors, first-order melting, vortex-glass, and Bose-glass transitions are predicted for different strength and types of disorder.¹ In the two-dimensional case, however, the theoretical picture has been that at finite temperature, in the presence of an arbitrary amount of disorder, there is no long-range translational order in the VL.² In this scenario, vortices are collectively pinned on length scales of the translational correlation length R_c and exhibit collective thermally activated motion at finite temperatures. However, in the absence of any disorder, the VL is expected to melt at a finite temperature via a dislocation mediated transition.³ This melting is progressive, however, beginning on long length scales and progressing to shorter length scales as the temperature increases above the melting temperature. In a previous paper,⁴ we have shown quantitative evidence that in the presence of weak pinning, melting in two-dimensional VL occurs locally on short length scales due to the dislocation unbinding mechanism. The "local melting" picture connects the theoretical views of collective pinning and two-dimensional melting by showing that the critical dynamics associated with melting is indeed cut off on long length scales due to the presence of disorder and the possibility of thermal activated creep in the VL.

In this paper, we present a more detailed study of the effect of disorder on this "local melting" phenomenon. By decreasing the sample thickness, thereby increasing the effect of disorder in the VL we show that the correlations in the VL decrease rapidly and eventually the local melting phenomenon disappears. As the influence of melting is reduced with increased disorder, thermal activated creep dominates the overall behavior of the VL.

In the absence of any disorder, the melting of the two-dimensional VL can occur as the solid phase becomes unstable to the unbinding of thermally created dislocation pairs. At the transition T_m , the long-wavelength shear modulus c_{66} is expected to drop abruptly to zero from a finite value satisfying the so-called universal jump ratio:

$$Ac_{66}a_0^2d/k_B T_m = 4\pi, \quad (1)$$

where a_0 is the lattice spacing, d is the sample thickness, and A is a factor ≤ 1 reflecting the renormalization of c_{66} by nonlinear lattice vibrations.⁵ Using the field dependence c_{66} as calculated by Brandt⁵ and known material parameters, the equation above can be used to calculate the phase diagram for the VL with A as the only free parameter. In addition to our previous study, there have been two other reports of experiments that have been interpreted as evidence for the melting of the two-dimensional VL.⁶ However, neither of these studies addressed the relevance of the disorder on the melting transition and its effect on the correlations in the VL. As we will show here, the effect of disorder can be strong enough so that the translational correlations in the vortex lattice are rather short and an observation of a melting transition is not possible. In this case, thermal activated creep can give rise to dynamical effects which are similar to but distinct from the melting behavior, and may be mistaken for melting.

The samples studied here are *a*-MoGe films grown by multitarget magnetron sputtering on sapphire substrates. Zero-field measurements have found the bulk penetration depth to be well described by the BCS dirty limit with a zero-temperature value of 7000 Å. The Ginzburg-Landau coherence length in these films is about 55 Å, which makes them extreme type-II superconductors. In calculating the phase diagram of the VL, we have used the previously measured slopes of the upper critical field on similar samples from transport studies.⁷ Here we contrast the results of the ac penetration depth measurement on samples with thickness 60, 300, 500, 1200, and 3000 Å. The strength of pinning varies from weak, in the 3000 Å film with $J_c \approx 10^2$ A/cm², to moderate in the 60 Å film $J_c \approx 10^4$ A/cm². For all the films, the characteristic bending lengths for vortices due to thermal fluctuations⁸ ($l_z \approx 8$ μm) and due to the pinning potential² ($l_c \approx 6$ μm) are much larger than the sample thickness, hence the VL in these samples is indeed two dimensional. As expected from the collective pinning theory, when samples are in the two-dimensional regime, the size of the correlation regions in the VL decreases with the sample thickness. When the pinning sites are randomly distributed, reducing the sample thickness d results in an increase of the pinning energy density for the vortices proportional to $1/\sqrt{d}$, while the VL elastic energy density remains unchanged. This results in a relative gain of energy for the pinned configuration of vortices, and hence in a smaller correlation area.

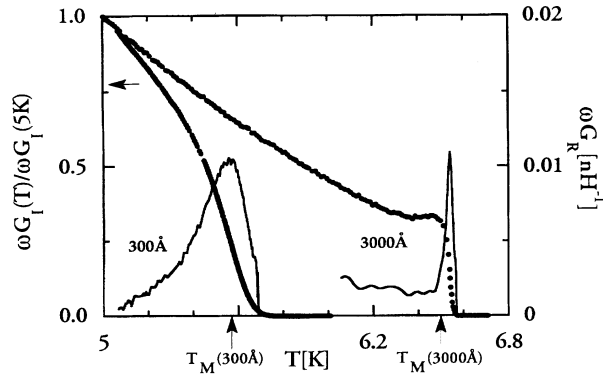


FIG. 1. Real and imaginary part of conductance for two different samples measured at 10 kHz in a 10 kOe field. The solid lines are the ωG_R and the solid circles are ωG_I scaled to their values at 5 K. The arrows at bottom show the calculated melting temperature for each sample (see text).

The experimental method used in this study is a two-coil mutual inductance measurement similar to that used by several groups to study vortex dynamics in superconducting films.^{9,10} The experimental configuration consists of a drive coil and an astatically wound pickup coil placed concentrically on the same side of the film. The drive coil induces an emf in the film which in turn produces shielding currents that are detected by the pickup coil. Using linear response theory, we can calculate the complex sheet conductance of the film from the measured in-phase and out-of-phase components of the induced currents. We used standard lock-in detection of the induced current and can easily verify the linearity of the response as well as study its frequency dependence. Using low frequencies and measuring at high temperatures where the real part of the sheet conductance is significant, we have demonstrated excellent agreement between the results of this technique with those of conventional four-probe resistivity measurements.⁴

In a thin film $d < \lambda$, the complex sheet conductance G is related to the generalized bulk complex ac penetration depth λ_{ac} : $\omega G = d/\mu_0 \lambda_{ac}^2$. Recent calculations by Coffey and Clem and by Brandt¹¹ show that in the presence of a large-enough field the complex conductance is dominated by the response of vortices. More specifically, they showed that below the melting transition in the vortex state the imaginary part of the sheet conductance ωG_I is a direct measure of the restoring force α_L due to pinning of the vortex system: $\omega G_I = d\alpha_L \phi_0 B$. The real part of the conductance is related to the dissipative motion of the vortices. The restoring force on the vortices, α_L , which can be inferred from the measured conductance, depends on the random pinning potential in the film as well as the elastic forces of the vortex lattice. In samples with weak disorder, as reported previously,⁴ the melting transition occurs with a sudden drop in ωG_I , corresponding to a sudden drop in α_L .

Figure 1 shows the behavior of $\omega G_I(T)/\omega G_I(5K)$ and ωG_R measured at 10 KHz for the 300 and 3000 Å films in a magnetic field of 10 kOe. The expected melting temperature of the VL for each film calculated using Eq. (1) with known material parameters and $A = 1$ are indicated by the arrows on the bottom of the figure. The real part of conductance ωG_R

of the 3000 Å film shows a sharp peak near the temperature where there is an abrupt drop in ωG_I . The drop of ωG_I signals an abrupt change of the restoring force α_L in the VL which occurs at a temperature close to the predicted melting temperature. The measured conductance on the 300 Å film, however, does not show any abrupt drop. While for this sample there is a relatively broad peak in ωG_R near the predicted melting temperature, the presence of a distinct melting transition is certainly not evident in ωG_I , i.e., in the restoring force. The conductance data on the various films measured show a gradual broadening of both the peak and the drop shown in Fig. 1 with decreasing sample thickness. We attribute this behavior to crossover between pinning and melting in the VL, pinning becoming more important at a given frequency as the film thickness is reduced. The data shown in Fig. 1 raise the question of whether the broad peak observed in the 300 Å film is due to a melting transition in the VL. The relation between the peak and the “local melting” transition can be made clear on the basis of the frequency dependence of the transition. We will show that a peak can occur due to either thermal activated creep of vortices or melting of the VL, depending on the frequency used to probe the vortices. We begin with the field dependence of the peak in ωG_R and its overall agreement with the melting scenario.

The field dependence of the peak in ωG_R observed near the predicted melting temperature at 10 kHz is shown in Fig. 2 for several of the samples studied here. Also shown (solid line) is the melting phase boundary calculated from Eq. (1) with $A = 1$, and the upper critical field $H_{c2}(T)$ determined from previous measurements on similar samples.⁷ Except at low fields, the overall shape of the field dependence is in very good agreement with the predicted melting phase boundary for the 1200 Å film and the 500 Å film. The 3000 Å film also shows equally good agreement but is not shown here. By contrast, the data on the 300 Å film follow the melting line at higher fields, but deviates strongly from the predicted melting line as temperature is increased and the peak moves to lower fields. The gradual broadening of the peak and the drop in ωG_I observed as the sample thickness is reduced accompanies the deviation of the peak position in ωG_R from the predicted melting temperature.

To further clarify the physical interpretation of these peaks and to demonstrate the crossover between pinning and melting, we consider the frequency dependence of our results. The frequency dependence also shows that the observed peaks in ωG_R are not caused by finite size effects, which can occur in general in ac experiments.¹¹ Changing the measurement frequency corresponds to probing the VL on various length scales: $l_\omega = \sqrt{D/\omega}$ where D is the characteristic diffusion constant in the VL. Figure 3 shows the frequency dependence of the peak in ωG_R measured for the 1200, 500, and 300 Å films in the presence of a 10 kOe field. The frequency dependence for all the films shows two regimes. The extent of each of the two regimes in frequency depends on the sample and the magnetic field. At low frequencies, which correspond to long length scales, we observe activated behavior for the temperature of the peak with the form $U/T_\omega = -\ln(\omega\tau)$ (dashed lines in Fig. 3). The activation energy extracted from this behavior is in good agreement (within 10%) with the activation energy extracted from

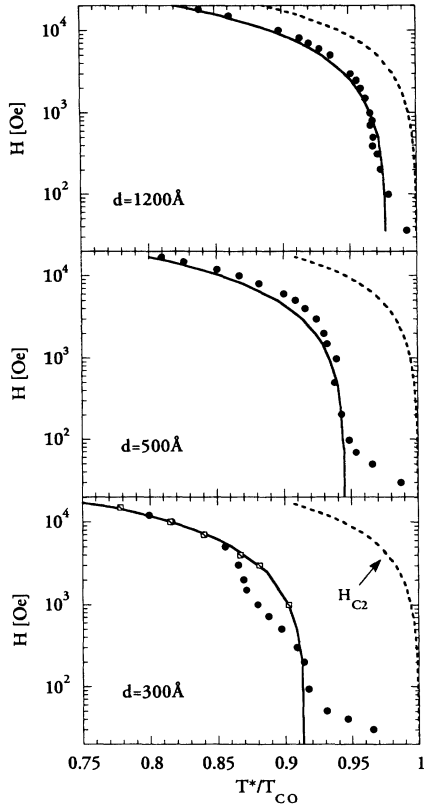


FIG. 2. Solid circles are the position of the peak in ωG_R in the H - T plane measured at 10 kHz. Square symbols shown only for the 300 Å film are a zero-frequency extrapolation from the high-frequency data (see text for an explanation). The solid lines are the melting lines calculated from Eq. (1) for each sample. The dashed lines are the H_{C2} for each sample (see text).

dc resistivity measurements on similar samples using standard four-probe measurements. These results suggest that at low frequencies the peak in ωG_R corresponds to the temperature at which the thermally activated relaxation time equals the effective measurement time ω^{-1} . At higher frequencies, however, the data are consistent with the critical dynamics of the two-dimensional melting as we have reported previously.⁴ The frequency dependence in this regime is determined by the divergence of the correlation length of the freezing VL as temperature is reduced. It has the form

$$\frac{T_\omega}{T_m} = 1 + \left[\frac{b}{\ln(\sqrt{\omega_0/\omega})} \right]^{2.71}, \quad (2)$$

where T_m is the melting temperature, $\omega_0 = \alpha D/a_0^2$ is the characteristic relaxation frequency of dislocations in the VL, b is a nonuniversal constant of order unity, and a_0 is the VL spacing. We used Eq. (2) with $b=0.6$, and $\omega_0(1200 \text{ \AA}) \approx 3 \times 10^{10} \text{ Hz}$, $\omega_0(500 \text{ \AA}) \approx 1 \times 10^9 \text{ Hz}$, and $\omega_0(300 \text{ \AA}) \approx 3 \times 10^8 \text{ Hz}$ to fit the high-frequency behavior for the three different samples for several fields. Figure 3 shows the frequency dependence for the samples in the presence of a 10 kOe field. It is interesting to note that the characteristic frequencies used in the fits are nearly equal to that of the vortex diffusion frequencies in the vortex liquid phase, estimated

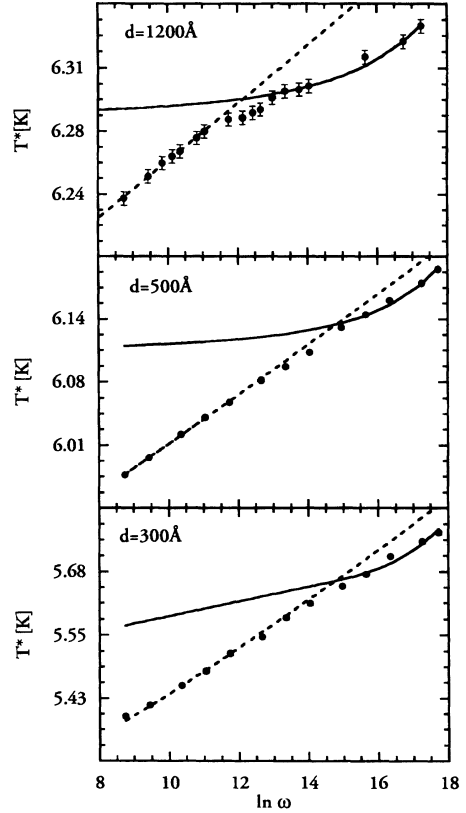


FIG. 3. Frequency dependence of the peak temperature for three different samples in presence of a 10 kOe field. Solid line is a fit to the dynamical theory [Eq. (2)] and the dashed line is a fit by an activated model.

from the measured resistance for each sample. Perhaps, the observed reduction in ω_0 with the sample thickness, can be attributed to the changes in the vortex diffusion caused by the increased strength of disorder in the VL. The melting temperatures $T_m(H)$, obtained from fits shown in Fig. 3, are in excellent agreement (within 1%) with the melting temperatures computed from Eq. (1) with $A=1$. The deviation from the melting dynamics and the crossover to an activated behavior at low frequencies shown in Fig. 3 reflects the cutoff of the spatial correlations by the presence of disorder in the VL. For each sample, we can identify a length scale R_ω associated with the cutoff in the freezing process by using the lowest frequency at which the melting dynamics is observed, ω_c , and the characteristic frequency, ω_0 , obtained from the fit at each field: $R_\omega/a_0 = \sqrt{\omega_0/\omega_c}$. This length scale represents the largest length over which the ac response of the vortex lattice is dominated by the diffusion of free dislocations near the melting temperature. Qualitatively, one might expect that this dynamical length is limited by the static correlation length R_c of the collective pinning theory. Previously, we have shown that the field dependence of R_ω is qualitatively consistent with that of R_c .⁴ Here we study the influence of the increased disorder with the reduction of the sample thickness by determining R_ω for all the samples in the presence of a particular magnetic field. In Fig. 4, we show the variation of this length with sample thickness at a fixed magnetic field of 10 kOe. Increasing disorder by means

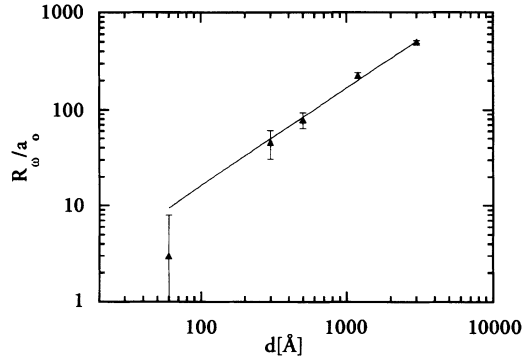


FIG. 4. Behavior of the crossover length (see text) which estimates the size of the correlation length in the VL for all the samples measured at 10 kOe. Solid line is a power-law fit to the data.

of decreasing the sample thickness, we find that the cutoff length R_ω is reduced rapidly. This reduction of R_ω is qualitatively consistent with the collective pinning theory, however, quantitatively $R_\omega \propto d$ which decreases faster than the predicted \sqrt{d} for R_c . It is important to note that presence of surface pinning which has been ignored in our discussion could in principle result in a faster decay of the correlations with sample thickness than that predicted by the collective pinning theory. For the thinnest film, the 60 Å film, we do not observe any melting, therefore we can only derive an upper bound $R_\omega < 3a_0$. The 60 Å film is in the regime with strong disorder in the VL, where the melting phenomenon is absent and thermal activated creep dominates the VL response on all length scales.

The static correlation length in VL R_c can be determined using critical current measurements and the results of collective pinning theory. Recently, transport measurements on similar films have been used to study the relation between the energy barriers for vortex motion and R_c .¹² While the activation energy and the magnetic field dependence of R_c and the length R_ω determined in this study are in good agreement, R_c is less than R_ω by a consistent factor of order of 10. This discrepancy is perhaps caused by the difference in the way each experiment probes the VL and the theoretical inaccuracies in determining the absolute value of the correlation length. Qualitatively, however, the overall behavior shown in Fig. 4 is consistent with the transport measurements and the collective pinning theory.

The consequence of the behavior of R_ω on the disorder established here is that for more strongly pinned films, one has to probe the VL at higher frequencies, i.e., shorter length scales, to observe local melting. The behavior of the 300 Å film exhibits this point clearly in Fig. 2, where the 10 kHz data fall well below the calculated melting line [Eq. (1)] for the intermediate values of the magnetic field, whereas, the extrapolated T_m based on the fits to the high-frequency data using Eq. (2) shown for a few fields (square symbols in Fig. 2) are in excellent agreement with the predicted melting temperature. We emphasize that for samples with a moderate amount of disorder, like the 300 Å film, it is crucial to study the frequency dependence response to distinguish between the dynamics of thermal activation and melting in the vortex state.

In conclusion, the effect of increased disorder in a two-dimensional VL is to rapidly shorten the extent of the correlated regions established near the melting temperature. We have studied this effect by probing the dynamics of vortex motion on various length scales in samples with different strengths of disorder/pinning. In the case of moderate disorder, we have shown that the dynamics of vortex motion near the melting temperature on length scales shorter than the translational correlation length R_c are consistent with a melting of vortices in a lattice. On long length scales, however, vortices in the two-dimensional VL exhibit collective thermal creep at finite temperature regardless of the amount of disorder.

Note added in proof. Another possible interpretation of the cutoff length R_ω is that this length is the dynamical equivalent of the orientational correlation length in the VL, R_0 , rather than a length associated with the translational correlation length, R_c . In fact, R_0 is a natural cutoff length scale for the dislocation unbinding dynamics since above this length dislocations in the VL dissociate to make free disclinations. Recent calculations by Toner [Phys. Rev. Lett. **66**, 2523 (1991) and **67**, 1810 (1991)] predict that $R_0 > R_c$ in the presence of weak disorder. More importantly, Toner predicts that these correlation lengths scale together such that $R_0 \propto R_c^2$. This result can account for the sizable difference between R_ω and R_c , if R_ω is taken as a dynamical measure of R_0 . This scenario also explains the observed thickness dependence of R_ω .

We thank Seb Doniach for helpful discussions. This work was supported by the Air Force Office of Scientific Research. A.Y. acknowledges financial support from IBM.

¹G. Blatter, M. V. Fiegl'man, V. B. Geshkenbein, A. I. Larkin, and V. M. Vinokur (unpublished).

²A. I. Larkin and Yu. Ovchinnikov, J. Low Temp. Phys. **34**, 409 (1979).

³B. A. Hubermann and S. Doniach, Phys. Rev. Lett. **43**, 950 (1979); D. S. Fisher, Phys. Rev. B **22**, 3519 (1980).

⁴A. Yazdani *et al.*, Phys. Rev. Lett. **70**, 505 (1993).

⁵E. H. Brandt, Phys. Status Solidi B **77**, 551 (1976).

⁶P. L. Gammel, A. F. Hebard, and D. J. Bishop, Phys. Rev. Lett. **60**, 144 (1988); P. Berghuis, A. L. F. van der Slot, and P. H.

Kes, Phys. Rev. Lett. **65**, 2583 (1990); P. Berghuis and P. H. Kes, Phys. Rev. B **47**, 262 (1993).

⁷J. M. Graybeal and M. R. Beasley, Phys. Rev. B **29**, 4167 (1984).

⁸D. R. Nelson, Phys. Rev. Lett. **60**, 1973 (1988).

⁹B. Jeaneret *et al.*, Appl. Phys. Lett. **67**, 386 (1989).

¹⁰A. F. Hebard and A. T. Fiory, Physica **109&110B**, 1637 (1982).

¹¹M. W. Coffey and J. R. Clem, Phys. Rev. Lett. **67**, 386 (1991); E. H. Brandt, *ibid.* **67**, 2219 (1991).

¹²W. R. White, A. Kapitulnik, and M. R. Beasley, Phys. Rev. Lett. **70**, 670 (1993).